Self-Compensated Insulating ZnO-Based Piezoelectric Nanogenerators

*Dohwan Kim, Keun Young Lee, Manoj Kumar Gupta, Subrata Majumder, and Sang-Woo Kim**

Remarkable enhancement of piezoelectric power output from a nanogenerator (NG) based on a zinc oxide (ZnO) thin film is achieved via native defect control. A large number of unintentionally induced point defects that act as n-type carriers in ZnO have a strong influence on screening the piezoelectric potential into a piezoelectric NG. Here, additional oxygen molecules bombarded into ZnO lead to oxygen-rich conditions, and the n-type conductivity of ZnO is decreased dramatically. The acceptor-type point defects such as zinc vacancies created during the deposition process trap n-type carriers occurring from donor-type point defects through a self-compensation mechanism. This unique insulating-type ZnO thin film-based NGs (IZ-NGs) generates output voltage around 1.5 V that is over ten times higher than that of an n-type ZnO thin film-based NG (around 0.1 V). In addition, it is found that the power output performance of the IZ-NG can be further increased by hybridizing with a p-type polymer (poly(3-hexylthiophene-2,5-diyl):phenyl-C_{61}-butyric acid methyl ester) via surface free carrier neutralization.

1. Introduction

Scavenging electrical energy from wasted mechanical energy resources has attracted extensive attention for powering portable devices with low operating power consumption and self-powered electronics. Piezoelectric nanogenerators (NGs) based on piezoelectric nanostructures and thin films have recently emerged as promising energy harvesters and have been adapted for various applications such as powering light-emitting diodes, liquid-crystal displays, and self-powered pH/pressure/light/speed sensors.[1–3] Among the various piezoelectric materials, zinc oxide (ZnO) exhibits several advantages for NG applications compared to lead-based piezoelectric materials due to its biocompatibility, relatively low band gap, superior optical properties, and easy synthesis process.[4–16]

D. Kim, Prof. S.-W. Kim
SKKU Advanced Institute of Nanotechnology (SAINT)
Center for Human Interface Nanotechnology (HINT)
Sungkyunkwan University (SKKU)
Suwon 440–746, Republic of Korea
E-mail: kimsw1@skku.edu

K. Y. Lee, Dr. M. K. Gupta, Dr. S. Majumder, Prof. S.-W. Kim
School of Advanced Materials Science and Engineering
Sungkyunkwan University (SKKU)
Suwon 440–746, Republic of Korea

DOI: 10.1002/adfm.201401998

Recent studies have demonstrated stable power-generating performance and mechanical durability of piezoelectric semiconductor and ferroelectric insulator thin films-based NGs.[17–20] However, the fabrication of high-performance flexible NGs based on insulating ferroelectric thin films, such as $BaTiO_3$ and $Pb(Zr,Ti)O_3$, which exhibit high piezoelectric charge coefficients[17,18] compared to semiconducting piezoelectric ZnO, is very limited because there is no available plastic substrate that can endure the high growth temperatures for high-quality ferroelectric thin films.[21,22] In this regard, complicated device fabrication processes such as thin-film transfer have been used to fabricate ferroelectric thin film-based NGs. However, we cannot be perfectly free from the formation of strain-induced defects such as ripples and cracks during the transfer process, which degrade the power-generating performance of NGs.

Without any intentional doping, ZnO exhibits n-type behavior from native defects such as donor-type oxygen vacancy (V_o), Zn interstitial (Zn_i), and the presence of H atoms.[23,24] In ZnO, V_o is a very common defect that plays an important role in screening the piezoelectric potential under mechanical deformation, resulting in only small piezoelectric potential-induced power output observed from n-type ZnO-based NG (NZ-NG).[25–27] However, the preparation of insulating/high-resistive ZnO has proven to be difficult because of its self-compensation[28] of the native point defects (such as V_o or Zn_i). The surface passivation of n-type conductive ZnO thin film using p-type polymer for improving the piezoelectric output power of NZ-NG has recently been reported in our previous reports.[17,18] However, improving the performance of the NZ-NG by controlling the donor type V_o and other defects without using any external passivation agent is a necessary but challenging task for increasing the output voltage/current and for future piezo-photonics applications.[29,30]

Here, we demonstrate high piezoelectric power generation from an insulating type (i-type) ZnO-based NG (IZ-NG). It was found that the formation of acceptor-type defects such as zinc vacancy (V_{Zn}) in the ZnO thin film due to additional oxygen incorporation during the radio-frequency (RF) sputtering process, which significantly improves the output performance of the NG. The piezoelectric output voltage and current density are

measured from a highly resistive IZ-NG under the application of forward bending conditions with 0.068% mechanical strain. Dramatic enhancement is observed in the output performance of the IZ-NG as compared to that of the NZ-NG. Furthermore, due to the compensation of donor defects including V_o in ZnO, piezoelectric screening is significantly prevented without using any passivation agent. The piezoelectric output voltage is further improved in IZ-NG by surface passivation of i-type ZnO using p-type poly(3-hexylthiophene) (P3HT) and phenyl-C_{61}-butyric acid methyl ester (PCBM) hybridized polymer. Due to the p-type polymer coated onto the i-type ZnO thin film, the remaining V_o and surface defects are further passivated, which further enhances the piezoelectric power output performance.

2. Results and Discussion

To demonstrate the self-compensation of donor-type defects such as V_o due to acceptor-type defects such as V_{Zn} in the ZnO crystal, two types of flexible piezoelectric NGs, NZ-NG and IZ-NG were fabricated using RF sputtering at room temperature. The proposed device consists of a piezoelectric i-type ZnO thin film grown on polyethylene naphthalate (PEN) substrate coated with flexible indium tin oxide (ITO). A thin layer of silver (Ag) with a thickness of 200 nm and a layer of molybdenum oxide (MoO_3) with a thickness of about 20 nm were coated on the top surface of ZnO thin film for Schottky contact formation, which served as the top electrode for the NG. A similar design and other parameters were also adopted for fabrication of the NZ-NG.

Initially, without using any external passivation agent such as P3HT onto the ZnO layer, the output voltage and current density were measured under the application of bending and releasing conditions from both IZ-NGs and NZ-NGs. **Figure 1** shows the piezoelectric output voltage and current density measurement from the NGs. For i-type ZnO (Figure 1b,d), the average output voltage and current density reached values up to 1.25 V and 3.10 μA cm^{-2}, whereas for n-type ZnO (Figure 1a,c), these values reached up to 0.10 V and 1.90 μA cm^{-2}, respectively, under the same application of bending conditions with mechanical strain of 0.068%. The small piezoelectric output voltage and current density from the NZ-NG are attributed to the screening effect caused by free electrons, donor defects, and surface defects present in the n-type ZnO. The high piezoelectric output voltage and current density observed from the IZ-NG are due to the passivation of donor-like native defects such as V_o presented in i-type ZnO.

In order to exploit the intrinsic conductivity in i-type ZnO and n-type ZnO thin films, Hall-effect measurements were performed on both samples (see Supporting Information Table S1). The results show that the n-type ZnO has typical n-type conductive properties with a high electron concentration of 1.03×10^{17} cm^{-3}, mobility of 0.76 cm^2 V^{-1} s^{-1}, and resistivity of 79.4 Ωcm. On the other hand, the i-type ZnO shows very high resistivity over 10^7 Ω cm compared to the n-type ZnO, but the other parameters could not be measured with Hall-effect measurements because of its high resistivity. To confirm the passivation of native donor defects in the i-type ZnO and the possible prevention of screening effects in the NG, two other types of i-type ZnO thin films were also grown on ITO-coated

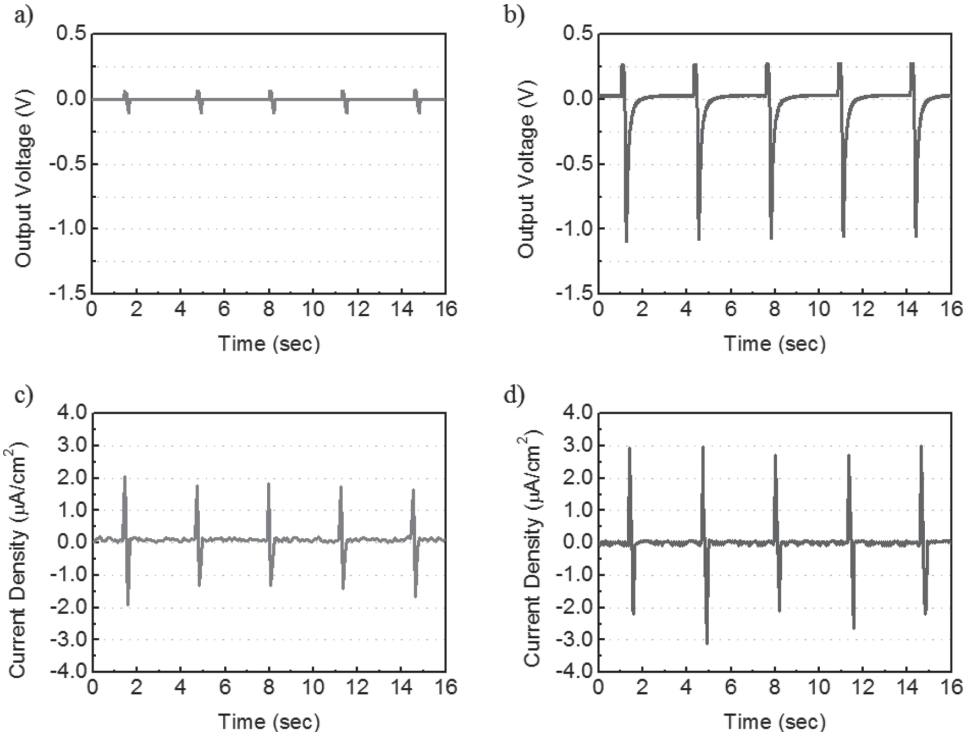

Figure 1. Measured piezoelectric power performance of ZnO thin-film-based nanogenerators under forward bending. Measured output voltage from a) NZ-NG (0.10 V) and b) IZ-NG (1.25 V). Measured current density from c) NZ-NG (1.90 μA cm^{-2}) and d) IZ-NG (3.10 μA cm^{-2}).

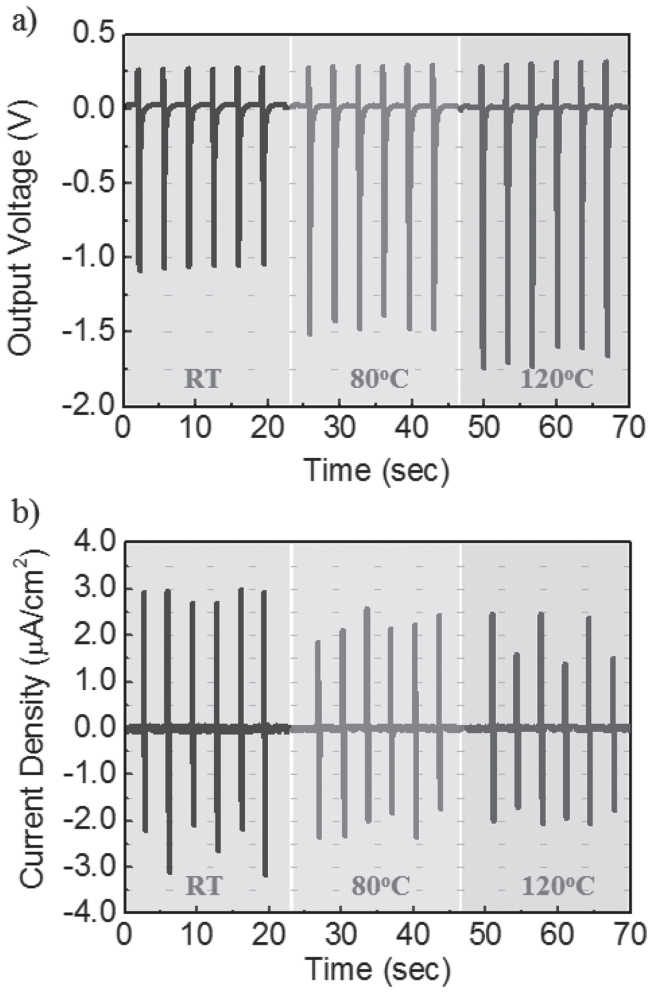

Figure 2. Measured piezoelectric power performance of IZ-NG grown with different substrate temperatures. a) Measured output voltage of IZ-NG (RT: 1.25 V, 80 °C: 1.52 V, and 120 °C: 1.74 V). b) Measured current density of IZ-NG (RT: 3.10 μA cm^{-2}, 80 °C: 2.60 μA cm^{-2}, and 120 °C: 2.50 μA cm^{-2}).

PEN substrates at different deposition temperatures of 80 °C and 120 °C by RF sputtering, keeping the same deposition parameters of O_2 and Ar gas flow rates and pressure similar to that deposited at room temperature (RT). The 80 °C and 120 °C grown IZ-NGs were then investigated for the piezoelectric output performance experiment.

The voltage and current density output from i-type ZnO TF-NGs were measured under bending and releasing conditions with 0.068% mechanical strain. **Figure 2**a shows the piezoelectric voltage output from three different IZ-NGs. With the increase of deposition temperature of the i-type ZnO, the piezoelectric output voltages also increase under the same mechanical deformation. The average output voltage increases from 1.25 V for RT to 1.52 V for 80 °C, and to 1.74 V for 120 °C successively. These output voltages obtained at RT, 80 °C and 120 °C are over one order higher than the output voltages observed for NZ-NG (0.10 V). The high piezoelectric output voltages from i-type ZnO thin films are attributed to the self-compensation of the intrinsic donor defects in the ZnO crystal

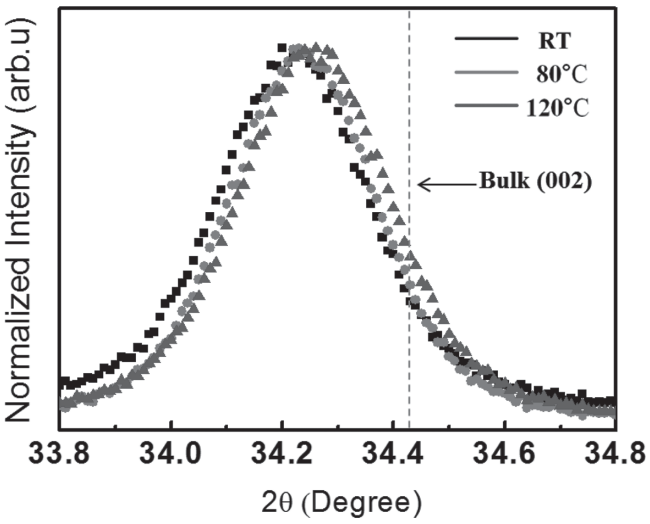

Figure 3. XRD patterns from the i-type ZnO thin films: (002) peaks are shifted toward the low 2θ side.

by simultaneously formed acceptor-type native defects under controlled deposition conditions. While output current density shows slight decrease as deposition temperature increase (RT: 3.10 μA cm^{-2}, 80 °C: 2.60 μA cm^{-2}, and 120 °C: 2.50 μA cm^{-2}) because the i-type ZnO becomes more intrinsic or highly resistive (Figure 2b). To understand the self-compensation and formation of acceptor-type native defects in i-type ZnO, detailed studies of X-ray diffraction (XRD), photoluminescence (PL) and X-ray photoelectron spectroscopy (XPS) were employed. XRD patterns from i-type ZnO thin films grown at RT, 80 °C, and 120 °C are shown in Supporting Information Figure S1.

A detailed analysis of the XRD spectra shows that the (002) phase peaks from these three i-type ZnO thin films are shifted towards lower 2θ from the standard bulk value (2$\theta \approx 34.42°$). More specifically, as the deposition temperature increases from RT to 120 °C, the value of 2θ also increases accordingly and approaches the bulk value, as shown in **Figure 3**. A similar peak shift with respect to the bulk ZnO value has been reported by previous researches and has been attributed to compressive strain.[31–33] It was proposed that the total compressive strain in the film is mainly attributed to the bombardment of neutralized/ionized oxygen sputtered from the ZnO target into the depositing ZnO thin film. Moreover, when additional oxygen gas (partial ratio ≈9%) is induced during the sputtering, many defects can be produced in the ZnO thin film by the incorporation of additional energetic oxygen atoms and negative oxygen ions (O^-).[33–35] Further, it was reported that acceptor-type V_{Zn} is mainly introduced by oxygen bombardment during sputtering.[36,37]

Further, in order to verify the presence of V_{Zn} and V_O defects inside the lattice of the ZnO crystal, PL studies have been carried out for n-type ZnO and all-i-type ZnO thin films. Each PL spectrum from the all-i-type ZnO thin films exhibits three main features. They all show a shoulder peak at 390 nm in the UV region, a high intensity peak at 405 nm in the violet region, and blue emission peaks at 435 nm and 485 nm (see **Figures 4**a–c). The observed weak emission peak at 390 nm arises in i-type ZnO thin films, which is associated with the

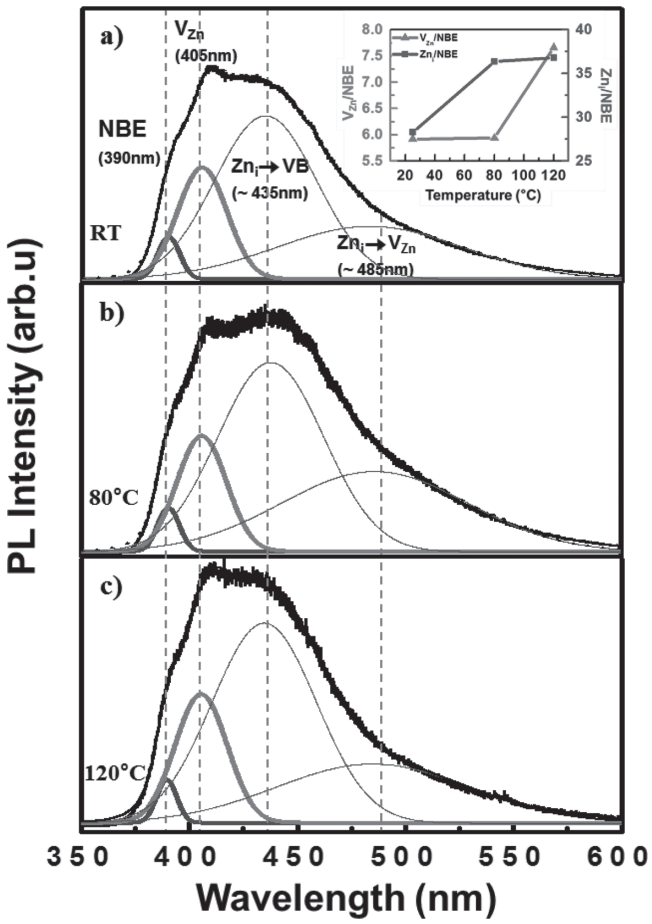

Figure 4. Photoluminescence emissions from i-type ZnO thin film grown at a) RT, b) 80 °C, and c) 120 °C. The inset represents the ratio dependencies of V_{Zn} to NBE (V_{Zn}/NBE) and Zn_i to NBE (Zn_i/NBE).

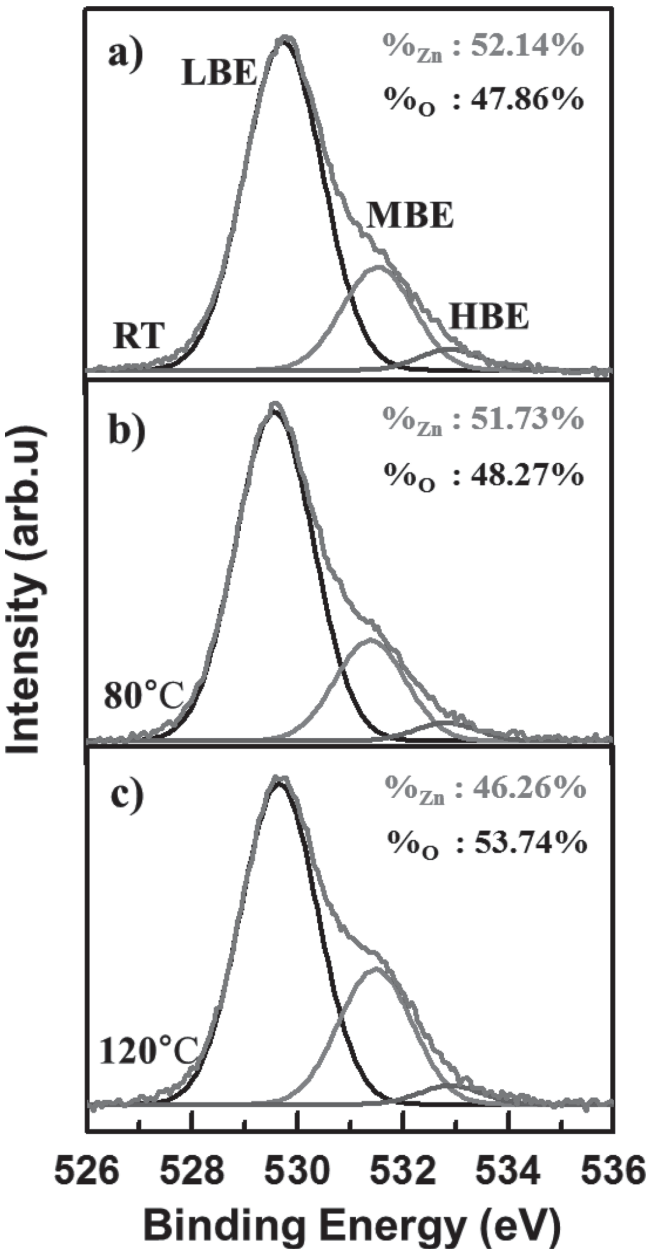

Figure 5. XPS data from i-type ZnO thin film grown at a) RT, b) 80 °C, and c) 120 °C.

near band-edge (NBE) emission,[38] whereas the emission peak at 405 nm is related to the acceptor-type V_{Zn} and originates from the electron transition from the conduction band edge to the V_{Zn} levels.[39] The broad violet luminescence around 450 nm is related to Zn_i (the electron transitions from Zn_i levels to the valence band (≈435 nm) and from Zn_i levels to V_{Zn} levels (≈485 nm)). However, in i-type ZnO thin films, no distinct emission bands are observed in the 540 to 600 nm region; these are usually observed in unintentionally doped n-type conductive ZnO, confirming the minute concentration of V_o in i-type ZnO thin films.[40,41] Therefore, we suggest that sufficient oxygen supply reduces the V_o concentration and increases the V_{Zn} and Zn_i concentrations at the same time. The PL results confirm the active passivation of donor-type V_o due to the self-formation of acceptor-type V_{Zn} in i-type ZnO thin films deposited at RT, 80 °C, and 120 °C.

To study the role of deposition temperature on the tendencies of V_{Zn} and Zn_i formation, ratios of V_{Zn} to the NBE (V_{Zn}/NBE) and Zn_i to NBE (Zn_i/NBE) were calculated on the basis of the corresponding integrated area of the emission band in PL spectra as shown in the inset of Figure 4. The V_{Zn}/NBE ratio increases from 5.92 for ZnO thin films deposited at RT to 5.94 for 80 °C and 7.66 for 120 °C, and a similar feature is also observed for the Zn_i/NBE ratio, which also increases from 28.31 for RT to 36.27 for 80 °C and 36.82 for 120 °C, implying that V_{Zn} and Zn_i increase with deposition temperature.

The increase in the concentration of VZn with the deposition temperature is also observed from the chemical state of ZnO investigated by XPS measurements. **Figure 5**a–c show the XPS spectra of O(1s) peaks from the three different samples of i-type ZnO thin films. Well-defined peaks corresponding to C(1s), O(1s), Zn($2p_{3/2}$), and Zn($2p_{1/2}$) elements are observed in the XPS spectra. The binding energies (BEs) are calibrated with respect to the C(1s) peak (284.6 eV) as a reference. The BE positions of Zn($2p_{3/2}$) and Zn($2p_{1/2}$) components are observed at 1.020 eV and 1.043 eV, respectively. The spin orbit splitting of these two

peaks for all three samples is shown at 23.0 ± 0.03 eV, corresponding to the 2p binding energy of Zn ions. Each of the O(1s) peaks of XPS spectra from three samples shows a composition of three distinct features, mainly the low BE (LBE), middle BE (MBE), and high BE (HBE) components centered at 529.7 eV, 531.5 eV, and 532.9 eV, respectively, as shown in the Figure 5.

The LBE component at 529.7 eV is attributed to O^{2-} ions surrounded by Zn in the ZnO compound system, serving as an indicator of the amount of oxygen atoms in a fully oxidized stoichiometric environment. The MBE component centered at 531.5 eV is associated with Ox^{-} ions ($x < 2$) in the oxygen-deficient regions within the ZnO matrix. The HBE component located at 532.9 eV can be typically attributed to the chemisorbed oxygen and dissociated oxygen or OH^{-} groups on the surface.[42–44] The deconvoluted O(1s) features for all i-type ZnO thin films are fitted using a function mixed with 80% Gaussian and 20% Lorentzian character. The corresponding areas are calculated for the three LBE, MBE, and HBE peaks, giving the total oxygen atomic concentrations of 47.86% at RT, 48.27% at 80 °C, and 53.74% at 120 °C. Clearly, these results imply the reduction of Zn concentration in the ZnO matrix with the increase of deposition temperature, indicating the formation of V_{Zn} sites inside i-type ZnO thin films. These XPS results are well correlated with the PL results.

To understand the influence of V_{Zn} on the piezoelectric output potential from an IZ-NG, we schematically illustrate the working principles of the NG under application of bending strain (**Figure 6**a–c). Figure 6 illustrates the auto-formation of donor and acceptor-like native defects in the i-type ZnO thin film by self-compensation. It is believed that many additional O atoms are both located in intrinsic and interstitials sites in the ZnO lattice without lattice distortion. An O atom at the intrinsic site removes V_o and form crystal structure (Figure 6a). An O atom at the interstitial site attracts near Zn atom, and thus creates V_{Zn} in the crystal structure (Figure 6b). Further, the attracted Zn atom and the interstitial O atom make an ionic pair with the created V_{Zn} and V_o, resulting in the electrically insulating property of the i-type ZnO thin film (Figure 6c).

When a compressive bending is applied to the IZ-NG, piezoelectric potential is less screened out in the IZ-NG due to the self-compensation of negatively charged donor defects, which is different from the severe compensation of piezoelectric potential in the NZ-NG. Thus, the piezoelectric charges generated into IZ-NG are greatly sustained, leading to dramatic enhancement of output voltage from the IZ-NG. **Figure 7**a,b show the piezoelectric output voltage signal for different bending directions (Figure 7a: forward bending, Figure 7b: reverse bending). Asymmetric and different output voltages under the forward and reverse bending situations are measured because of the strain rate difference occurring from pre-induced compressive stress of the *i*-type ZnO thin film.[45] In forward bending of IZ-NG, a sharp signal (I) is detected under compressive strain, and a broad peak signal (II) is detected when the strain is released. Since the thin film has native compressive stress, it is easy to induce a strain in the same direction, and therefore a weak peak is detected (Figure 7a–I). However, in the case of the releasing condition, since the strain releasing direction is opposite to the native compressive strain, it needs more force to return to its original state, and as a result, a strong peak is detected (Figure 7a–II). On the other hand, for reverse bending, a strong peak is detected in compressive conditions due to the opposite direction of applying strain and the native compressive strain of the thin film (Figure 7b–I). For a similar reason, a relatively weak peak is detected when it is released (Figure 7b–II).

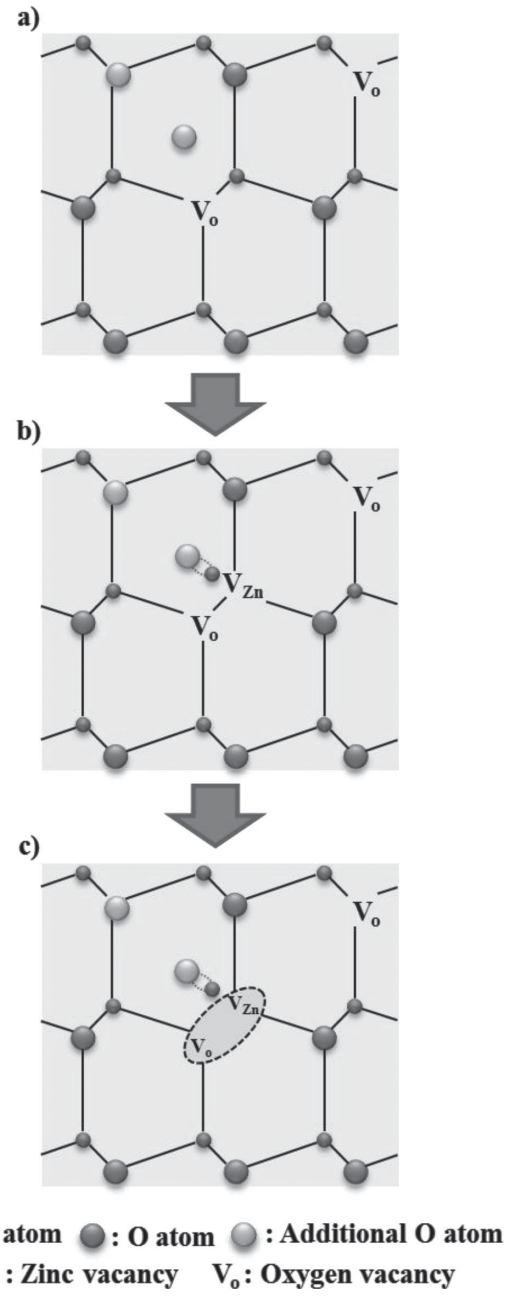

Figure 6. Schematic illustration of i-type ZnO thin film. a) Additional O atoms are both located in intrinsic and interstitials sites of ZnO lattice crystal. An O atom at intrinsic site removes V_o and form crystal structure. b) An O atom at the interstitial site attracts near Zn atom and creates V_{Zn} in the crystal structure. c) V_{Zn} and V_o make an ionic pair that is similar to an electron and hole pair, and thus ZnO is finally neutralized.

Moreover, it has been noted that the piezoelectric screening effect is not only caused by the donor defect, but also by the presence of surface defects and free electrons in ZnO.[14,15]

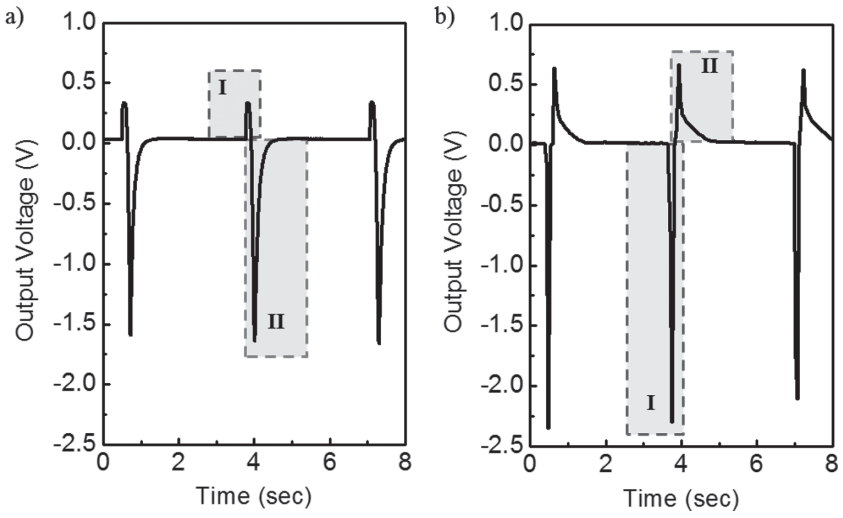

Figure 7. Measured output voltage under a) forward bending condition (1.57 V) and b) reverse bending condition of IZ-NG (2.40 V). Under compressive stress (I), there is a sharp signal, and under the releasing of stress (II) broad peak signals are detected.

At this stage, we also demonstrate the power enhancement in i-type ZnO by neutralizing the possible surface defects/electrons via p-type polymer. To demonstrate further output enhancement from the IZ-NG, we conjugated p-type polymers on an i-type ZnO thin film. We used hybridized polymers (P3HT:PCBM) to trap the free carriers at the surface, which leads to the possible reduction of the screening effect. The output power generation from three different P3HT:PCBM conjugated IZ-NG is measured under the forward bending conditions with mechanical strain of 0.068%. Output performance up to 1.66 V (3.75 μA cm^{-2}), 2.13 V (3.40 μA cm^{-2}), and 2.40 V (3.25 μA cm^{-2}) were obtained from polymer conjugated IZ-NGs deposited at RT, 80 °C, and 120 °C, respectively, as shown in **Figure 8**a,b. It is clear that the output power increases further due to the p-type polymer conjugation compared to the pristine IZ-NG. The enhancement in the output voltage is due to the increase in the piezoelectric potential via neutralization (passivation) of the free electrons in the ZnO thin film by attracting holes from P3HT and p-n junction formation.

3. Conclusion

We have demonstrated significant power output enhancement from ZnO thin film-based piezoelectric NG via native defect control. The average output voltage and current density reached values up to 1.25 V and 3.10 μA cm^{-2}, respectively, from the IZ-NG, whereas the values reached up to 0.10 V and 1.90 μA cm^{-2}, respectively, from the NZ-NG under the same application of bending conditions with mechanical strain of 0.068%. It was found that the small piezoelectric output voltage and current density from the NZ-NG are attributed to the screening effect caused by free electrons, donor defects, and surface defects present in the n-type ZnO. On the other hand, the larger power generation from the IZ-NG without additional passivation agents is due to the self-compensation of donor and acceptor type native defects. In addition, it was confirmed that the power performance of IZ-NG can be further increased by hybridizing with p-type polymer via the passivation of surface free carriers.

4. Experimental Section

A sputtered ZnO thin film was produced by an RF-magnetron sputtering system on a clean ITO electrode (thickness: 200 nm) deposited on a PEN film (thickness: 200 μm) and glass microscope slides. A power of 80 W was used to create the plasma with 9 mTorr of working pressure and different argon-oxygen mixture ratios (20:0 sccm for NZ-NG and 20:2 sccm for IZ-NG) and different substrate temperatures (RT, 80 °C, and 120 °C). Thin layers of Ag with a thickness of 200 nm and MoO_3 with a thickness of about 20 nm were coated on the top surface of ZnO thin film for Schottky contact formation, which served as the top electrode for the NG. A similar design and parameters were also adopted for the fabrication

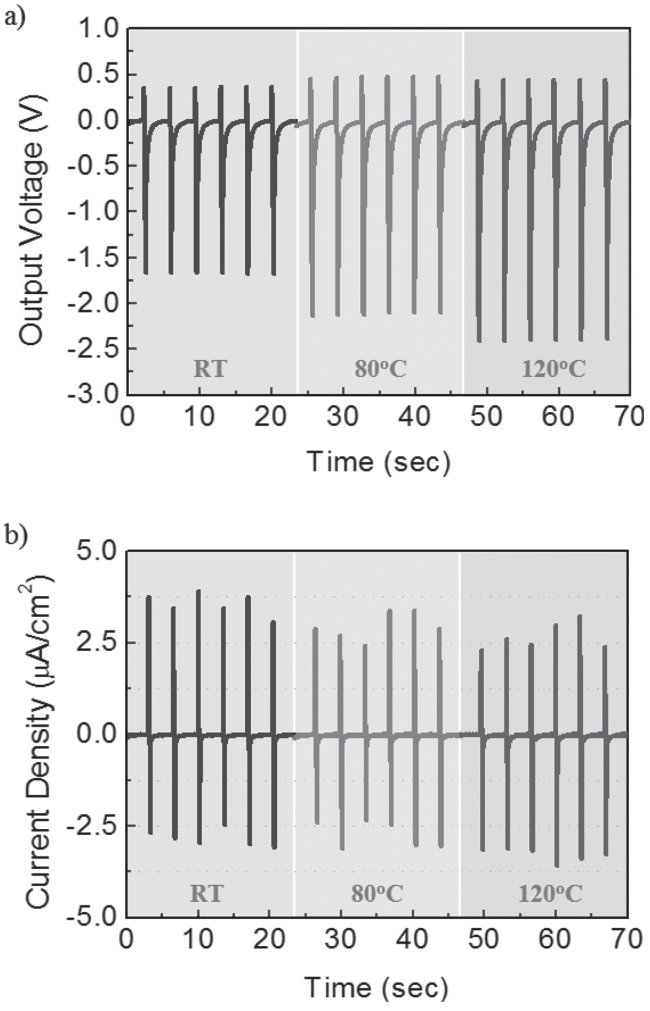

Figure 8. Power performance from P3HT:PCBM hybridized IZ-NG with different deposition temperatures with a) output voltage of 1.66 V at RT, 2.13 V at 80 °C, and 2.40 V at 120 °C and b) current density 3.75 μA cm^{-2} at RT, 3.40 μA cm^{-2} at 80 °C, and 3.25 μA cm^{-2} at 120 °C.

of an NZ-NG. The output voltage and current density were measured with a bending tester used to create a bending strain. A Keithley 6485 picoammeter and 2082A voltmeter were used to measure the low-noise current and output voltage generated by IZ-NG and NZ-NGs.

Supporting Information

Supporting Information is available from the Wiley Online Library or from the author.

Acknowledgements

This research was supported by the National Research Foundation of Korea (NRF) funded by the Ministry of Science, ICT & Future Planning (Grants 2012R1A2A1A01002787 and 2009–0083540) and by the Energy International Collaboration Research & Development Program of the Korea Institute of Energy Technology Evaluation and Planning funded by the Ministry of Knowledge Economy (Grant 2011–8520010050).

Received: June 17, 2014
Revised: July 31, 2014
Published online: September 12, 2014

[1] E. Cross, *Nature* **2004**, *432*, 24.
[2] S. Xu, Y. Qin, C. Xu, Y. Wei, R. Yang, Z. L. Wang, *Nat. Nanotechnol.* **2010**, *5*, 366.
[3] Z. L. Wang, *Adv. Mater.* **2011**, *24*, 279.
[4] M.-Y. Choi, D. Choi, M.-J. Jin, I. Kim, S.-H. Kim, J.-Y. Choi, S. Y. Lee, J. M. Kim, S.-W. Kim, *Adv. Mater.* **2009**, *21*, 2185.
[5] D. Choi, M.-Y. Choi, W. M. Choi, H.-J. Shin, H.-K. Park, J.-S. Seo, J. Park, S.-M. Yoon, S. J. Chae, Y. H. Lee, S.-W. Kim, J.-Y. Choi, S. Y. Lee, J. M. Kim, *Adv. Mater.* **2010**, *22*, 2187.
[6] S. N. Cha, J.-S. Seo, S. M. Kim, H. J. Kim, Y. J. Park, S.-W. Kim, J. M. Kim, *Adv. Mater.* **2010**, *22*, 4726.
[7] S. Xu, Y. Qin, C. Xu, Y. Wei, R. Yang, Z. L. Wang, *Nat. Nanotechnol.* **2010**, *5*, 366.
[8] Z. L. Wang, *Adv. Mater.* **2011**, *24*, 279.
[9] B. Kumar, S.-W. Kim, *Nano Energy* **2012**, *1*, 342.
[10] H.-K. Park, K. Y. Lee, J.-S. Seo, J.-A Jeong, H.-K. Kim, D. Choi, S.-W. Kim, *Adv. Funct. Mater.* **2011**, *21*, 1187.
[11] S. Lee, S.-H. Bae, L. Lin, Y. Yang, C. Park, S.-W. Kim, S. N. Cha, H. Kim, Y. J. Park, Z. L. Wang, *Adv. Funct. Mater.* **2013**, *23*, 2445.
[12] K.-H. Kim, B. Kumar, K. Y. Lee, H.-K. Park, J.-H. Lee, H. H. Lee, H. Jun, D. Lee, S.-W. Kim, *Sci. Rep.* **2013**, *3*, 2017.
[13] T. T. Pham, K. Y. Lee, J.-H. Lee, K. H. Kim, K. S. Shin, M. K. Gupta, B. Kumar, S.-W. Kim, *Energy Environ. Sci.* **2013**, *6*, 841.
[14] C. Pan, L. Dong, G. Zhu, S. Niu, R. Yu, Q. Yang, Y. Liu, Z. L. Wang, *Nat. Photonics* **2013**, *7*, 752.
[15] C. Pan, R. Yu, S. Niu, G. Zhu, Z. L. Wang, *ACS Nano* **2013**, *7*, 1803.
[16] R. Yu, C. Pan, J. Chen, G. Zhu, Z. L. Wang, *Adv. Funct. Mater.* **2013**, *23*, 5868.
[17] K. Y. Lee, B. Kumar, J.-S. Seo, K.-H. Kim, J. I. Sohn, S. N. Cha, D. Choi, Z. L. Wang, S.-W. Kim, *Nano Lett.* **2012**, *12*, 1959.
[18] S. Y. Chung, S. Kim, J.-H. Lee, K. Kim, S.-W. Kim, C.-Y. Kang, Y. S. Kim, *Adv. Mater.* **2012**, *24*, 6022.
[19] W. Wu, C. Pan, Y. Zhang, X. Wen, Z. L. Wang, *Nano Today* **2013**, *8*, 619.
[20] K.-I. Park, S. Xu, Y. Liu, G.-T. Hwang, S.-J. L. Kang, Z. L. Wang, K. J. Lee, *Nano Lett.* **2010**, *10*, 4939.
[21] X. Wang, C.-N. Xu, H. Yamada, K. Nishikubo, X.-G. Zheng, *Adv. Mater.* **2005**, *17*, 1254.
[22] J. Kim, S. A. Yang, Y. C. Choi, J. K. Han, K. O. Jeong, Y. J. Yun, D. J. Kim, S. M. Yang, D. Yoon, H. Cheong, K.-S. Chang, T. W. Noh, S. D. Bu, *Nano Lett.* **2008**, *8*, 1813.
[23] D. C. Look, G. C. Farlow, P. Reunchan, S. Limpijumnong, S. B. Zhang, K. Nordlund, *Phys. Rev. Lett.* **2005**, *95*, 225502.
[24] C. G. Van de Walle, *Phys. Rev. Lett.* **2000**, *85*, 1012.
[25] Y. Hu, L. Lin, Y. Zhang, Z. L. Wang, *Adv. Mater.* **2011**, *24*, 110.
[26] J. I. Sohn, S. N. Cha, B. G. Song, S. Lee, S. M. Kim, J. Y. Ku, H. J. Kim, Y. J. Park, B. L. Choi, Z. L. Wang, J. M. Kim, K. Kim, *Energy Environ. Sci.* **2013**, *6*, 97.
[27] X. Xue, Y. Nie, B. He, L. Xing, Y. Zhang, Z. L. Wang, *Nanotechnology* **2013**, *24*, 225501.
[28] D. C. Look, K. D. Leedy, L. Vines, B. G. Svensson, A. Zubiaga, F. Tuomisto, D. R. Doutt, L. J. Brillson, *Phys. Rev. B* **2011**, *84*, 115202.
[29] F. Zhang, Y. Ding, Y. Zhang, X. Zhang, Z. L. Wang, *ACS Nano* **2012**, *6*, 9229.
[30] F. Zhang, S. Niu, W. Guo, G. Zhu, Y. Liu, X. Zhang, Z. L. Wang, *ACS Nano* **2013**, *5*, 4537.
[31] R. Kumar, N. Khare, V. Kumar, G. L. Bhalla, *Appl. Surf. Sci.* **2008**, *254*, 6509.
[32] P. R. Benger, K. Chang, P. Bhattacharya, J. Singh, K. K. Bajaj, *Appl. Phys. Lett.* **1988**, *53*, 684.
[33] P. Patsalas, C. Gravalidis, S. Logothetidis, *J. Appl. Phys.* **2004**, *96*, 6234.
[34] M. D. McCluskey, S. J. Jokela, *J. Appl. Phys.* **2009**, *106*, 071101.
[35] R. Hong, H. Qi, J. Huang, H. He, Z. Fan, J. Shao, *Thin Solid Films* **2005**, *473*, 58.
[36] X. Wen, J. A. Davis, L. Van Dao, P. Hannaford, V. A. Coleman, H. H. Tan, C. Jagadish, K. Koike, S. Sasa, M. Inoue, M. Yano, *Appl. Phys. Lett.* **2007**, *90*, 221914.
[37] D. Kim, J. Yang, J. Hong, *J. Appl. Phys.* **2009**, *106*, 013908.
[38] Y. Chen, D. M. Bagnall, H. J. Koh, K. T. Park, K. Hiraga, Z. Q. Zhu, T. Yao, *J. Appl. Phys.* **1998**, *84*, 3912.
[39] S.-H. Jeong, B.-S. Kim, B.-T. Lee, *Appl. Phys. Lett.* **2003**, *82*, 2625.
[40] U. Ilyas, R. S. Rawat, T. L. Tan, P. Lee, R. Chen, H. D. Sun, Li Fengji, S. Zhang, *J. Appl. Phys.* **2011**, *110*, 093522.
[41] A. Janotti, C. G. V. Walle, *Rep. Prog. Phys.* **2009**, *72*, 126501.
[42] M. Chen, X. Wang, Y. H. Yu, Z. L. Pei, X. D. Bai, C. Sun, R. F. Huang, L. S. Wen, *Appl. Surf. Sci.* **2000**, *158*, 134.
[43] Z. G. Wang, X. T. Zu, S. Zhu, L. M. Wang, *Phys. E* **2006**, *35*, 199.
[44] K. G. Saw, K. Ibrahim, Y. T. Lim, M. K. Chai, *Thin Solid Films* **2007**, *515*, 2879.
[45] R. S. Yang, Y. Qin, L. M. Dai, Z. L. Wang, *Nat. Nanotechnol.* **2009**, *4*, 34.